# Experimental and theoretical investigation of the contact fatigue behaviour of an epoxy polymer under small amplitude sliding micro-motions

Marie-christine Baïetto-dubourg, Antoine Chateauminois

# EXPERIMENTAL AND THEORETICAL INVESTIGATION OF THE CONTACT FATIGUE BEHAVIOUR OF AN EPOXY POLYMER UNDER SMALL AMPLITUDE SLIDING MICRO-MOTIONS

M.C. DUBOURG[1] and A. CHATEAUMINOIS[2]

*1 - Laboratoire de Mécanique des Contacts, UMR 5514, INSA de Lyon, 69622 Villeurbanne, France*

*2 - Laboratoire de Physico-Chimie Structurale et Macromoléculaire, UMR 7615, ESPCI, 75005, Paris, France*

## ABSTRACT

The cracking behaviour of a DGEBA/IPD epoxy material contacting a rigid glass sphere has been investigated under small amplitude cyclic micro-motions, i.e. fretting loading. Under predominantly elastic contact conditions, the initial damage within the epoxy counterface was found to be associated with the propagation of two main cracks at the edge of the contact and along two symmetrical locations with respect to the sliding direction. *In situ* visualisation of the contact interface also revealed a transition from fatigue to brittle propagation as the crack length increased. A theoretical contact mechanics modelling indicated that the cracks were initiated under predominantly mode I opening conditions and along an initial orientation close to the experimental one. A subsequent theoretical investigation of the crack response was carried out, which took into account the frictional response of the crack faces under the cyclic contact loading. The results demonstrated that, using the known bulk toughness of the epoxy, the calculated transition from fatigue to brittle failure was consistent with the experimental observations.

## KEYWORDS

Contact fatigue, epoxy, fretting, nucleation, propagation, toughness

## INTRODUCTION

Various semi-quantitative macroscopic fatigue wear models have been largely derived in order to account for the wear resistance of polymers substrates sliding against rigid counterfaces which are insufficiently rough for the elastic limit of the polymer to be exceeded during micro-asperity deformation [1-3]. These theoretical approaches were focused on the prediction of the wear resistance of tribological systems, but little attention was paid to the

identification of the fatigue wear damage mechanisms and their relationships with the polymer bulk mechanical properties. Direct experimental evidence of contact fatigue processes, however, are scarce: propagating cracks in polymers are difficult to detect on a micro-asperity scale because of the elastic recovery. As a result, the exact nature of the contact damage micro-mechanisms (brittle or fatigue failure) and the manner they relate to the toughness or fatigue properties remain largely unestablished. In a previous investigation [4], we have demonstrated that macroscopic contacts between glassy polymers and glass counterfaces, can be used as model 'single-asperity' contacts simulating, at an observable scale, the damage micro-mechanisms which may be induced at the micro-asperity level in real contacts between rough surfaces. Under small amplitude cyclic tangential micromotions (i.e. fretting), specific contact loading conditions can be selected which ensure that superficial fatigue cracking of the polymer substrate is the main induced damage. Using the in situ contact visualisation, these failure processes can be monitored under a well-controlled contact stress environment, which is an essential prerequisite for any attempt to correlate the contact damage to the bulk materials properties. Although the complex deformation conditions in the contact zone do not necessarily realise those which are addressed in 'conventional' mechanical testing, the relatively mild strain and strain rates encountered under fretting conditions make it realistic to establish some relationships between the observed cohesive wear damage processes and the bulk failure properties.
In the present investigation, the experimental contact fatigue behaviour of an epoxy resin contacting a rigid glass sphere has been analysed in the light of a theoretical contact mechanics approach focused on the prediction of the location and the initial orientation of the cracks induced under the cyclic frictional loading. A modelling of the crack propagation stages was also carried out in order to investigate crack arrest mechanisms and possible transitions from fatigue to brittle response.

## MATERIALS AND EXPERIMENTAL TECHNIQUES

### *Materials*

The polymer under investigation was an epoxy thermoset obtained by curing a stoichiometric mixture of diglycidyl ether of bisphenol (DGEBA) and isophoron diamine (IPD). The DGEBA and IPD monomers were supplied by CIBA (LY556, Switzerland) and by Hülls (Germany), respectively. After degassing under vacuum, the reactive mixture was poured into 30x30x5 $mm^3$ PTFE moulds and cured into an oven 2 h 30 at 140°C followed by 15 mn at 165°C. The physical and mechanical properties of the resulting material are reported in Table I. During crosslinking, one of the specimen's faces was directly exposed to air. The resulting mirror-like surface was subsequently used in the fretting tests. All the specimens were kept in a desiccator before use.
A smooth (r.m.s. roughness less than 2 nm) glass hemisphere with a 48 mm radius was used as a counterface. It was obtained by polishing cubic specimens 10x10x12 $mm^3$ of E glass (Vetrotex International, Chambery). Before use, the glass specimens were cleaned using ethanol and heated at 630°C for 1 hour in order to remove any organic contamination which could result from the polishing procedure.

Table I Mechanical properties of the DGEBA/IPD epoxy network.
(a) Quasi-static Young's modulus measured by Hertzian indentation; (b) Data taken from ref [5]; (c) Measured by Dynamic Mechanical Thermal Analysis (D.M.T.A) at 1 Hz ($T_\alpha$ is taken as the temperature of the maximum in tan δ); (d) $\sigma_y^u$ and $\sigma_y^p$ are the yield stress under uniaxial and plane strain compression, respectively, for an equivalent strain rate of $5x10^{-4}$ $s^{-1}$ (see ref [6] for details on the experimental procedure).

| E (GPa)[a] | $K_{IC}$ MPa.$m^{1/2}$ [b] | $T_\alpha$ (°C)[c] | tan δ (25°C)[c] | $\sigma_y^u$ (MPa)[d] | $\sigma_y^p$ (MPpa)[d] |
|---|---|---|---|---|---|
| 2.8 | 1.20 | 165 | 0.005 | 107 | 135 |

*Fretting tests*

The fretting-wear tests were carried out using a modified tension-compression hydraulic device (Fig. 1). The flat epoxy specimens were rubbed against the glass spherical caps under a constant applied normal load, P = 100 N. An oscillating tangential displacement in the range ±10 μm to ± 60 μm was imposed to the contacting specimens. The frequency of the associated triangular shaped signal was set to 1 Hz. During the fretting tests, the tangential load, Q, and the relative displacement, δ, were continuously recorded in order to obtain the so-called Q = f(δ) fretting loops. The relative displacement was measured using a high precision extensometer located close to the contact in order to minimize the effects of machine compliance. These data were used as an input in a real-time feedback loop which ensured the constancy of the amplitude of the imposed relative displacement throughout the test. *In situ* visualization of the contact interface was carried out through the glass counterface in a light transmission mode using a microscope device and a CCD camera. For the contact conditions under consideration, the measured diameter of the contact area, 2a, was 2.1 mm, which yielded an average contact pressure $p_m$ = 32 MPa.

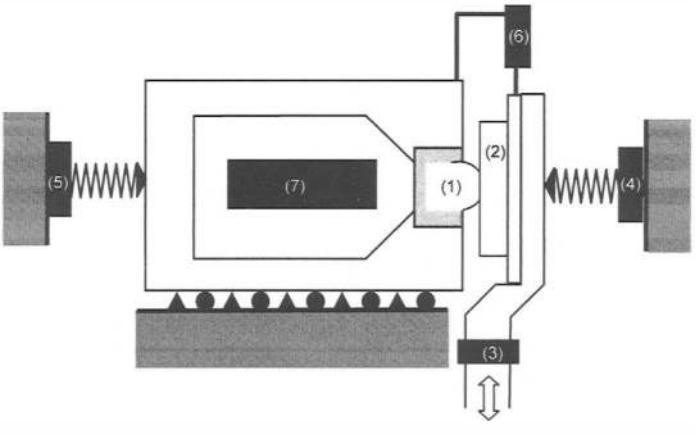


Fig. 1 Schematic description of the fretting device. *(1)* spherical glass counterface, *(2)* epoxy specimen, *(3)* tangential load transducer, *(4,5)* normal load transducers, *(6)* extensometer, *(7)* microscope and CCD camera.

## RESULTS AND DISCUSSION

*Determination of the contact conditions*

Fretting loading is associated with complex contact conditions which are characterized by the occurrence of either partial slip conditions or gross slip conditions, depending on the contact loading (normal load, imposed displacement), the elastic properties of the contacting bodies and the frictional response of the contact interface (coefficient of friction). Under partial slip conditions, the contact area is characterised by the existence of a central adhesive zone (no slip) surrounded by an external micro-slip annulus. In contrast, micro-slip is distributed over the whole contact area under gross slip conditions. The precise identification of these contact conditions has been shown to be crucial for the analysis of the associated contact damage and the determination of the necessary boundary conditions in any contact mechanics modelling [7, 8]. In a previous investigation [9], the fretting conditions of the contact under investigation have been analysed as a function of the normal load, the imposed displacement and the number of fretting cycles. On the basis of these results, the present investigation will be focused on the analysis of the cracking mechanisms which occur within the gross slip regime, i.e. for displacement amplitudes greater than ± 40 μm under a 100 N normal load.
A first stage in the analysis consisted in determining the elastic or plastic nature of the contact loading using the known yield properties of the bulk DGEBA/IPD system. The latter were established experimentally assuming that they obey a modified Von Mises criterion taking into account the effect of the hydrostatic pressure. This criterion may be written as:

$$\tau_{oct} = \tau_{octo} + \alpha P \tag{1}$$

where $\tau_{oct}$ and P are the octahedral shear stress and the hydrostatic pressure respectively, which can be expressed, in terms of the principal stresses as :

$$\tau_{oct} = \frac{1}{3}\left[(\sigma_1 - \sigma_2)^2 + (\sigma_1 - \sigma_3)^2 + (\sigma_2 - \sigma_3)^2\right]^{1/2} \tag{2}$$

$$P = -\frac{1}{3}(\sigma_1 + \sigma_2 + \sigma_3) \tag{3}$$

In equation (1), $\tau_{octo}$ corresponds to the shear yield stress under zero pressure and $\alpha$ is a pressure coefficient, which quantifies the yield stress sensitivity to pressure. Such a yield criterion has previously been shown to hold for epoxy resins under a wide range of pressure, temperature and strain rate conditions [10, 11]. The two parameters, $\tau_{octo}$ and $\alpha$ were found to be 44 MPa and 0.173 respectively from the uniaxial and plane strain compression results reported in table I.
The distribution of octahedral shear stress and pressure within the contact has been calculated from the explicit theoretical expressions of the contact stresses beneath a rigid sliding sphere which were derived by Hamilton [12]. As reported in reference [9], the coefficient of friction, $\mu$, increases slightly during the early stages of the fretting process. The maximum, stabilised, value ($\mu$ = 1.2) was taken into account for the present calculation. The calculated stress profiles are reported in Figure 2, at the surface of the epoxy specimen and along a direction orthogonal to the sliding direction, where the maximum values of the octahedral shear stress are likely to occur. These results indicate that the contact remains loaded elastically during sliding, except within a narrow region located at the edge of the contact. It must, however, be noted that the yield stress criterion was established, for practical reasons, at an equivalent

strain rate of $5x10^{-4}$ $s^{-1}$, while the strain rates within the epoxy surface layer are in the order of $10^{-2}$ $s^{-1}$ under fretting conditions. Accordingly, the values of the octahedral shear stress at the onset of yield are probably underestimated. In addition to the limited viscoelastic response of the epoxy material at the considered frequency and temperature (tan $\delta$ = 0.005 at 25°C and 1 Hz, table I), this analysis supports the validity of a global elastic description of the contact stress environment.

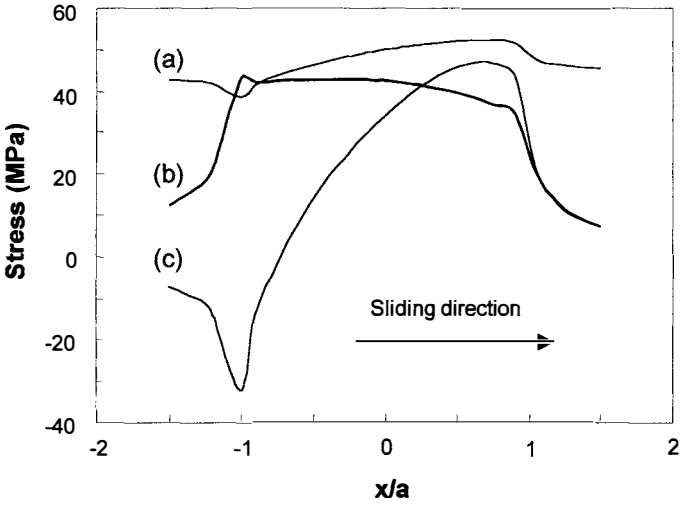


Fig.2 Profiles of *(a)* the limit octahedral shear stress at yield, *(b)* the octahedral shear stress and *(c)* the hydrostatic pressure at the surface of the epoxy specimen and along the sliding direction (a is the radius of the contact area).

*In situ analysis of the initial damage mechanisms*

A typical example for the development of a contact fatigue crack network is shown in Figure 3. *In situ* visualisation showed that, after about 300 fretting cycles, two cracks nucleated at the edge of the contact and at two approximately symmetrical locations along the sliding direction. During about 100 fretting cycles, crack propagation occurred in progressive, fatigue like manner. When a critical length (between 200 µm and 400 µm) was reached, brittle propagation occurred. During this final brittle propagation stage, a strong decrease in the contact tangential stiffness, K, was observed. As indicated in Figure 3, K was measured from the initial linear slope of the fretting loop, i.e. during the incipient stages of the tangential loading. Under such conditions, the contact stiffness is essentially a function of the contact diameter and the elastic shear response of the contacting bodies [13]. As no significant change in the size of the contact area was noted during crack propagation, the strong drop in K can thus be attributed to the reduced resistance of the epoxy body to tangential displacement, due to the crack opening processes induced by the tangential loading. This was supported by *post-mortem* microscope observation of specimens cross sections (Fig. 3), which showed that the depth of the two main cracks at the edge of the contact (up to 900 µm, i.e. the order of magnitude of the contact radius)) allowed significant crack opening mechanisms. The monitoring of the contact stiffness therefore suggests that substantial changes in the contact stress field are induced during the propagation of the two main cracks. The initial growth

direction of these cracks was found to be about 11° with respect to the normal to the surface. It did not change very appreciably with the propagation depth.

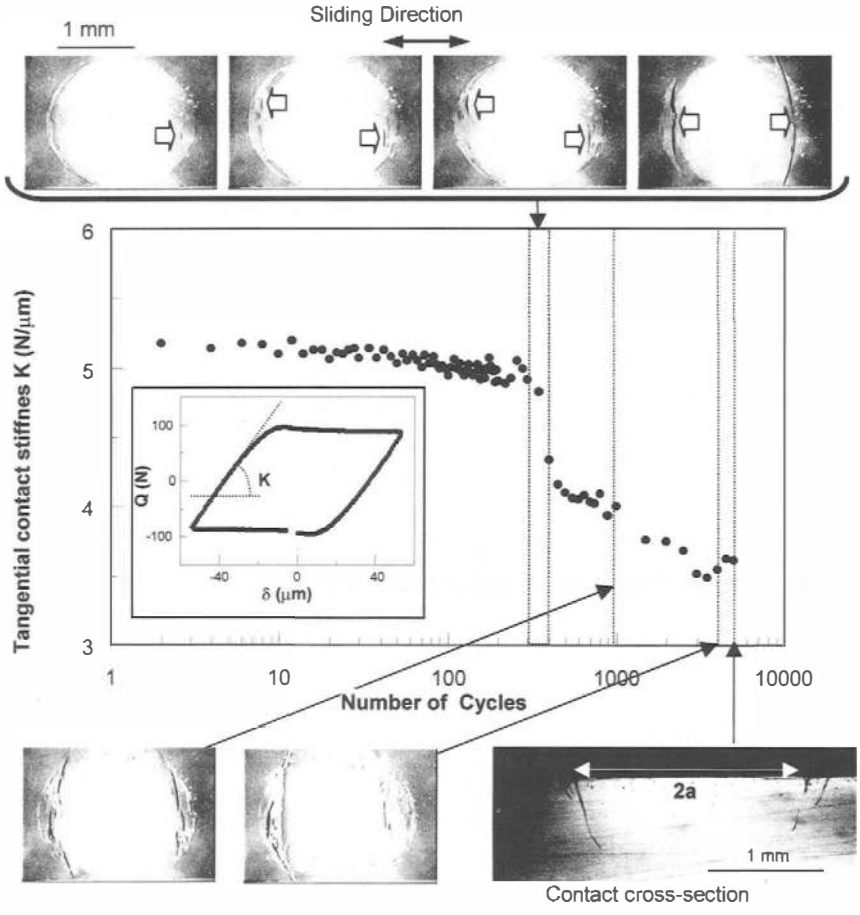


Fig. 3 Crack initiation and propagation processes in the gross-slip regime. Pictures (except bottom right) are taken from *in situ* visualisation of the contact. The arrows indicate the location of the cracks.

As the number of fretting cycles was increased, secondary cracks developed close to the initial cracks, but they resulted in a more limited and progressive decrease in the contact stiffness. After the propagation of the initial main cracks, their neighbouring areas are unloaded as a consequence of crack opening during the tangential loading. These processes can account for the limited propagation of the secondary cracks.

*Theoretical analysis of the location and orientation of cracks*

In a first stage, the theoretical analysis of the cracking processes was directed toward the prediction of the location of the cracks and their initial orientation with respect to the surface. This analysis was carried out using a two steps procedure. At first, the contact problem was solved as a unilateral contact problem obeying a Coulomb's friction law. By means of a Kalker's algorithm [14], the contact area, the contact pressure distribution and the internal stresses were determined under a gross-slip contact condition. The magnitude of the tangential load was determined from the experimental value of the coefficient of friction within the gross slip regime ($\mu = 1.2$). In a second stage, the initial crack propagation processes were analysed in the meridian plane of the contact, $y = 0$ (Fig. 4), where the cracks first initiate. The crack initiation mechanisms have been considered theoretically in the light of a simple dislocation dipole model which was initially introduced for metallic materials [15, 16]. Parameters based on the amplitude of the shear stress, $\tau_m$, along a particular direction and the amplitude of the tensile stress, $\sigma_m$, perpendicular to this direction, have been considered to derive the crack initiation criterion. In order to take into account the strong stress gradient close to the contact interface, $\tau_m$ and $\sigma_m$ have been averaged over a finite length (4 μm) from the polymer surface. As detailed in a previous paper using aluminium alloys [17], the choice of these parameters can be justified from well established physical arguments based on the growth of dislocations from the surface of the crystalline materials. Within the context of this study, the parameters based on $\tau_m$ and $\sigma_m$ will be used without underlying assumption regarding the nature of the microscopic processes involved in crack initiation within the glassy amorphous epoxy. As a first approach, they will just be used as mechanical parameters which allows discriminating between predominant mode I and mode II crack propagation driving forces.

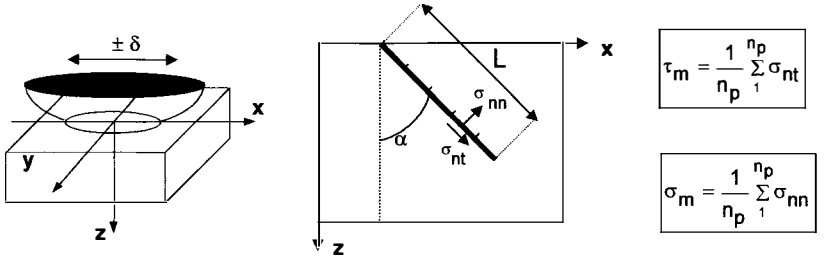


Fig. 4 Theoretical modelling of crack initiation. Calculation of the average shear ($\tau_m$) and tensile ($\sigma_m$) stresses as a function of crack orientation, $\alpha$, with respect to the contact plane.

For various discrete steps of the cyclic tangential loading, the values of $\tau_m$ and $\sigma_m$ have been calculated for different orientations, $\alpha$, with respect to the normal to the surface and for different locations (x,z) within the meridian plane. In Figure 5a, the maximum value, $\Delta\sigma_m^*$, of the effective amplitude of the average tensile stress on the surface ($z = 0$) of the epoxy specimen has been reported as a function of the orientation. $\Delta\sigma_m^*$ is defined as the amplitude of the *positive* values of the average tensile stress ($\sigma_m > 0$), which are assumed to represent the driving force regarding the opening of tensile cracks. In the same figure, the orientation, $\alpha^*$, of the plane corresponding to the maximum amplitude of the effective average tensile stress has also been reported. Due to the loading symmetry and for the sake of clarity, only the results corresponding to one half of the contact have been represented. The results shows that the maximum amplitude of $\sigma_m$ occurs at the edge of the contact ($x/a = -1$) and along an

orientation, $\alpha^* = 7°$, which is very close to the experimental initial crack propagation direction (11°). The calculated value of $\alpha^*$ was found to be roughly independent on the depth up to 50 μm, while the amplitude of $\Delta\sigma_m^*$ decreased from about 70 MPa to 60 MPa within the same range (Fig. 5b).

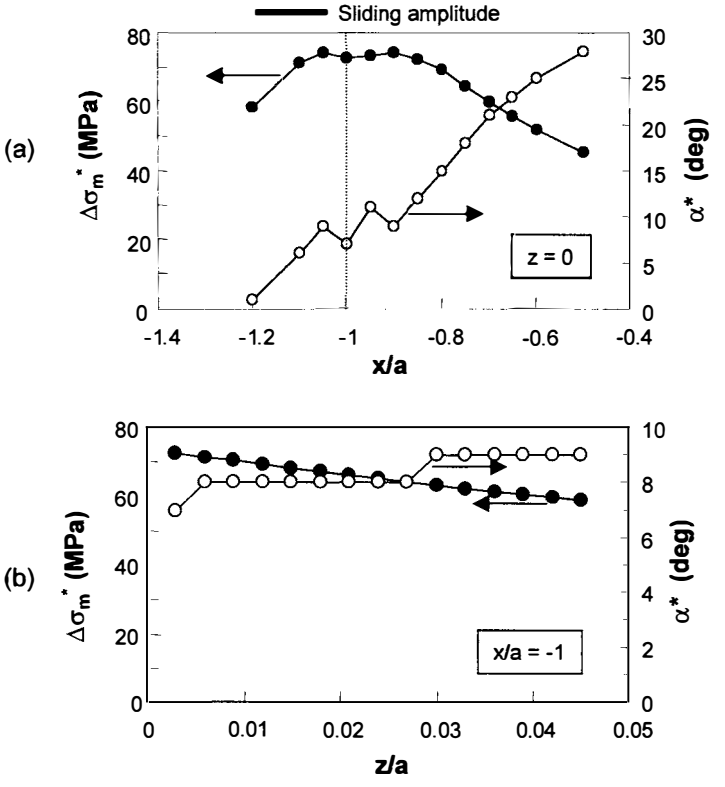


Fig. 5 Maximum amplitude of the average effective tensile stress, $\Delta\sigma_m^*$, and orientation, $\alpha^*$, of the corresponding plane as a function of *(a)* the location within the contact interface; z = 0 *(b)* the depth, z, for x/a = -1.

The calculations also showed that, at the edge of the contact, the maximum amplitude of the shear stress, $\Delta\tau_m$, was minimised along the direction corresponding to the maximum tensile stress amplitude (Fig. 6). The combined analysis of $\Delta\sigma_m^*$ and $\Delta\tau_m$ therefore establishes that the main cracks which nucleate close to the contact edge correspond to predominantly tensile (mode I) fatigue cracks. In addition, the distribution of $\Delta\sigma_m^*$ within the contact plane can interestingly be considered (Fig. 7). The maximum amplitude of the tensile stresses is located within two croissant shaped areas oriented perpendicular to the sliding direction, which corresponds to the regions were crack initiation was observed experimentally for the various tests carried out under gross slip condition.

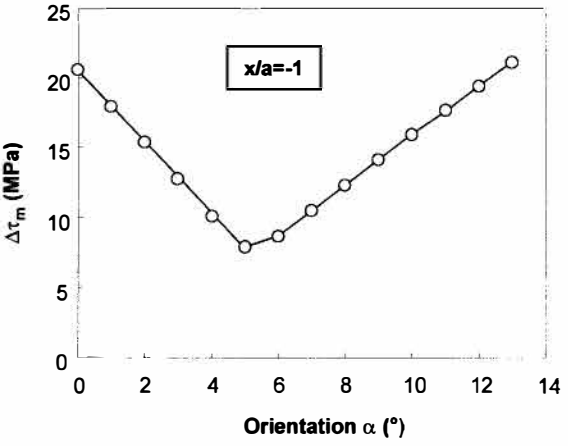


Fig. 6 Change in the maximum amplitude of the shear stress, $\Delta\tau_m$, at the edge of the contact (x/a = -1, z = 0) as a function of the orientation, α.

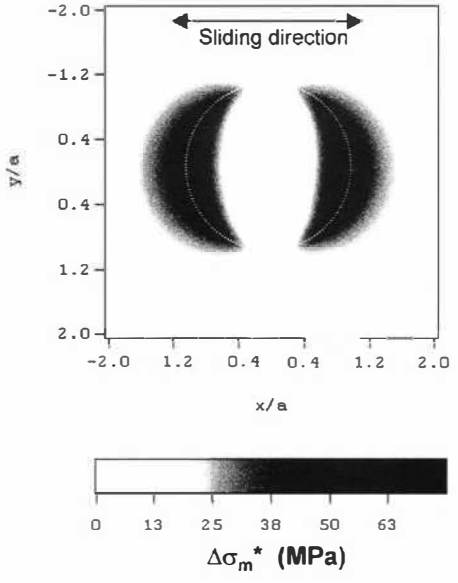


Fig.7 Distribution of the maximum amplitude of the tensile stress, $\Delta\sigma_m$*, in the contact plane (z = 0). The dotted circle delimits the contour of the contact area.

*Analysis of crack propagation*

The second part of the investigation was directed toward the understanding of the crack propagation stages. Two questions were especially addressed: *(i)* the determination of the transition from fatigue to brittle fracture *(ii)* the determination of the crack arrest conditions. Within the frame of linear elastic fracture mechanics, such an analysis requires the

determination of the stress intensity factors at the crack tip, which are dependent on the contact conditions at the crack interface. It is therefore of importance to determine whether the cracks faces are in contact or not and whether they slide with respect to each other.

This analysis was undertaken within the frame of a general model developed by Dubourg and Villechaise [18-20]. This theoretical two-dimensional linear elastic approach of multiple frictional contact fatigue cracks allows us to determine the stress and displacements fields in cracked solids and the associated stress intensity factors $K_I$ and $K_{II}$. The model is based upon a modified dislocation theory and on the resolution of the contact problem between crack faces as a unilateral contact with friction. Stress and displacement fields are given by superimposing the individual responses of the uncracked solid and of the cracks to the contact loading in a manner that satisfies the boundary conditions along the faces of the cracks. The continuum stress field within the uncracked solid is obtained numerically from the above-mentioned Kalker's algorithm. The crack response is associated with displacement discontinuities along its faces, opening and slip, which generate stresses. These displacement zones are modelled using continuous distributions of dislocations. For more details on the model, the reader should refer to refs [18-20].

The analysis was carried out in the contact meridian plane ($y = 0$) where a single straight crack located at $x/a = -1$ and oriented to 7° with respect to the normal to the surface was considered. This simplified description of the crack geometry was justified by the observation that their orientations did not change greatly as a function of depth. As a first order approximation, the unknown coefficient of friction between the crack faces was assumed to be equal to 0.6. The crack behaviour and the associated stress intensity factors during the various discrete steps of the cyclic tangential loading are represented in Figure 8. During the alternate tangential loading, opening (steps 1 to 3) and closing (steps 4 to 6) mechanisms of the crack were simulated in accordance with the *in situ* observation of the crack dynamics. Interestingly, the simulation also predicts the occurrence of some sliding at the tip of the closed crack (steps 5 and 6), which demonstrates *a posteriori* the necessity of taking into account the tribological behaviour of the crack faces. The calculation of $K_I$ and $K_{II}$ also clearly demonstrates the complex non-proportional loading of the crack tip, which complicates any quantitative comparison of the stress intensity factors with the bulk toughness data obtained under pure mode I or mode II conditions.

In Figure 9 the maximum calculated values of $K_I$ and $K_{II}$ have been reported as a function of the crack length. As the maximum values of $K_I$ and $K_{II}$ do not necessarily occur at the same time during the cyclic loading, it is not obvious how to quantify the level of mode mixity from these data. It can, however, be noted that $K_I$ is the preponderant stress intensity factor over the whole range of crack lengths, which confirms the predominantly tensile nature of the observed cracks. As the crack length is increased, the maximum value of $K_I$ goes up to values slightly higher than the experimental fracture toughness ($K_{IC}$ = 1.2 MPa $m^{1/2}$, ref [5]). Accordingly, the simulation predicts a transition from fatigue to brittle crack propagation, which is consistent with the above reported *in situ* observations. Taking into account the experimental toughness, this transition should occur for a crack depth close to 200 µm. The corresponding experimental value was not available, but it was observed that the length of the cracks at the surface of the epoxy specimens at the onset of brittle propagation (between 200 µm and 400 µm) was of the same order of magnitude. For crack lengths greater than 250 µm, a progressive decrease in the maximum value of $K_I$ is calculated. For a crack length of about 400 µm, this value is lowered below $K_{IC}$, which corresponds to crack arrest conditions for brittle propagation. The observed maximum crack lengths at the end of the fretting tests were, however, about twice the predicted critical length for crack arrest. This discrepancy could be attributed to the occurrence of some additional sub-critical fatigue propagation after the brittle propagation stage, to the effects of mode mixity or to an insufficient description of the

frictional behaviour of the crack faces, which could affect the calculation of stress intensity factors.

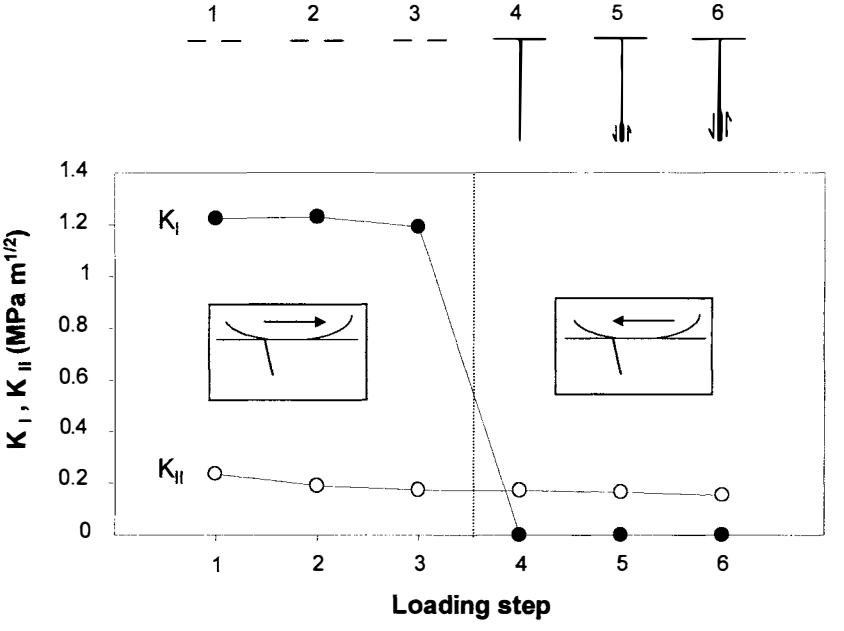


Fig. 8 Theoretical description of the crack behaviour and calculated values of $K_I$ and $K_{II}$ during the discrete steps of a cyclic tangential loading (crack depth : 350 μm).

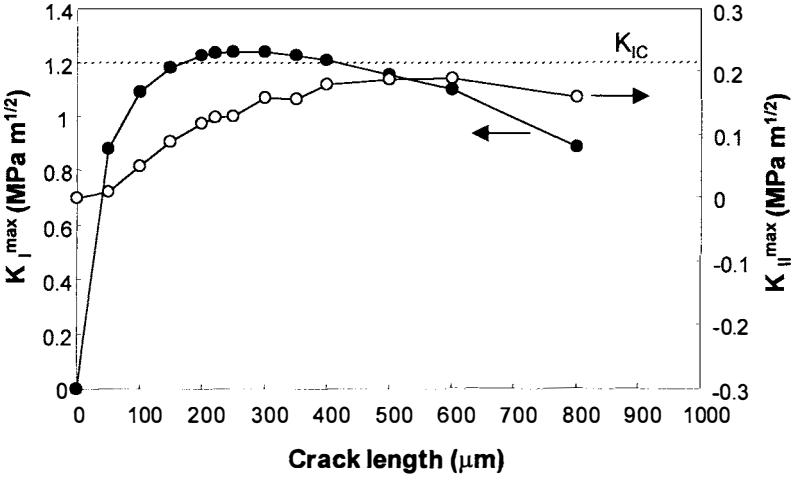


Fig. 9 Maximum calculated values of $K_I$ and $K_{II}$ as a function of crack depth.(the dotted line corresponds to the experimental bulk fracture toughness).

## CONCLUSION

The cyclic damage behaviour of a DGEBA/IPD epoxy resin contacting a smooth glass hemisphere under fretting conditions was found to be associated with the nucleation and the propagation of two deep cracks at the edge of the contact. From a theoretical modelling of the elastic contact stresses, it was possible to ascribe these cracking mechanisms to predominantly mode I opening mechanisms. A theoretical analysis of the crack behaviour under the contact induced stress field also allowed determination of the changes in the stress intensity factors, $K_I$ and $K_{II}$, as a function of the crack length. Despite the non-proportional nature of the mixed-mode crack tip loading, the comparison of the calculated $K_I$ values to the experimental toughness properties of the epoxy allowed a reasonable description of the observed transition from fatigue to brittle propagation as the crack length increased. This investigation therefore supports the validity of a fracture mechanics approach of contact fatigue processes within glassy amorphous polymers.

## ACKNOWLEDGEMENT

A. Chateauminois wishes to thank C. Gauthier (GEMPPM, INSA de Lyon, France) for her help in measuring the yield properties of the epoxy system.

## REFERENCES

1 Jain, V. K. and Bahadur, S. (1980) *Wear* **60**, 237.
2 Jain, V. K. and Bahadur, S. (1982) *Wear* **79**, 241.
3 Lancaster, J. K. (1990) *Wear* **141**, 159.
4 Chateauminois, A., Kharrat, M. and Krichen, A. (2000). *Analysis of Fretting Damage in Polymers by Means of Fretting Maps*, ASTM STP 1367, pp.325-366, Chandrasekaran, V. and Elliott, C. B., Eds, West Conshohocken.
5 Urbaczewski-Espuche, E., Galy, J., Gerard, J. F., Pascault, J. P. and Sautereau, H. (1991) *Pol. Eng. Sci.* **31**, 1572.
6 Quinson, R., Perez, J., Rink, M. and Pavan, A. (1997) *J. Mat. Sci.* **32**, 1371.
7 Vincent, L. (1994) *Materials and fretting.*, in ESIS 18, Mech Eng Pub, pp.323-337, London.
8 Fouvry, S., Kapsa, P. and Vincent, L. (1996) *Wear* **200**, 186.
9 Kharrat, M., Chateauminois, A. and Krichen, A. (1999).*Trib Tran* **42**, 377.
10 Lesser, A. J. and Kody, R. S. (1997) *J. Polym. Sci. B: Polym. Phys.* **35**, 1611.
11 Kody, R. S. and Lesser, A. J. (1997) *J. Mat. Sci.* **32**, 5637.
12 Hamilton, G. M. (1983) *Proc. Inst. Mech. Eng.* **197C**, 53.
13 Johnson, K. L. (1985). *Contact Mechanics*. Cambridge University Press, Cambridge.
14 Kalker, J. J. (1990). *Three dimensional elastic bodies in rolling contact*. Kluwer Academic Publishers, Dordrecht.
15 Tanaka, K. and Mura, T. (1981) *J. Appl. Mech.* **47**, 111.
16 Yamashita, N. and Mura, T. (1983) *Wear* **91**, 235.
17 Lamacq, V. and Dubourg, M. C. (1999) *Fatigue & Fracture of Eng. Mat. and Struct.* **22**, 535.
18 Dubourg, M. C. and Villechaise, B. (1992) *ASME J. Trib.* **114**, 462.
19 Dubourg, M. C. and Villechaise, B. (1989) *Eur. J. Mech. A* **8**, 309.
20 Dubourg, M. C. and Villechaise, B. (1992) *ASME J. Trib.* **114**, 455.